



UNITED STATES AIR FORCE
ARMSTRONG LABORATORY

**Long Term Effects of Retinal Laser
Lesions: Multifocal ERGs
(Electroretinogram) and Vernier Visual
Evoked Potentials (VEPs)**

Elmar T. Schmeisser

TASC, Inc.
4241 Woodcock Drive, Suite B-100
San Antonio, TX 78228

19980410 067

March 1998

Approved for public release;
distribution is unlimited.

Occupational and Environmental Health
Directorate
Optical Radiation Division
8111 18th Street
Brooks Air Force Base TX 78235-5215

NOTICES

When Government drawings, specifications, or other data are used for any purpose other than in connection with a definitely Government-related procurement, the United States Government incurs no responsibility or any obligation whatsoever. The fact that the Government may have formulated or in any way supplied the said drawings, specifications, or other data, is not to be regarded by implication, or otherwise in any manner construed, as licensing the holder or any other person or corporation; or as conveying any rights or permission to manufacture, use, or sell any patented invention that may in any way be related thereto.

The mention of trade names or commercial products in this publication is for illustration purposes and does not constitute endorsement or recommendation for use by the United States Air Force.

The Office of Public Affairs has reviewed this report, and it is releasable to the National Technical Information Service, where it will be available to the general public, including foreign nationals.

This report has been reviewed and is approved for publication.

Government agencies and their contractors registered with Defense Technical Information Center (DTIC) should direct requests for copies to: Defense Technical Information Center, 8725 John J. Kingman Rd, Ste 0944, Ft. Belvoir, VA 22060-6218.

Non-government agencies may purchase copies of this report from: National Technical Information Service (NTIS), 5285 Port Royal Road, Springfield VA 22161-2103.

Leon N. Mclin, Jr.
LEON N. MCLIN, JR., Lt Col, USAF
Chief, Optical Radiation Division

REPORT DOCUMENTATION PAGE

Form Approved
OMB No. 0704-0188

Public reporting burden for this collection of information is estimated to average 1 hour per response, including the time for reviewing instructions, searching existing data sources, gathering and maintaining the data needed, and completing and reviewing the collection of information. Send comments regarding this burden estimate or any other aspect of this collection of information, including suggestions for reducing this burden, to Washington Headquarters Services, Directorate for Information Operations and Reports, 1215 Jefferson Davis Highway, Suite 1204, Arlington, VA 22202-4302, and to the Office of Management and Budget, Paperwork Reduction Project (0704-0188), Washington, DC 20503.

1. AGENCY USE ONLY (Leave blank)	2. REPORT DATE	3. REPORT TYPE AND DATES COVERED	
	March 1998	Final - September 1995 to June 1997	
4. TITLE AND SUBTITLE			5. FUNDING NUMBERS
Long Term Effects of Retinal Laser Lesions: Multifocal ERGs (Electroretinogram) and Vernier Visual Evoked Potentials (VEPs)			C - F33615-92-C-0017 PE - 62202F PR - 7757 TA - 02 WU - 99
6. AUTHOR(S)			
Elmar T. Schmeisser			
7. PERFORMING ORGANIZATION NAME(S) AND ADDRESS(ES)			8. PERFORMING ORGANIZATION
TASC 4241 Woodcock Drive Suite B-100 San Antonio, TX 78228			
9. SPONSORING/MONITORING AGENCY NAME(S) AND ADDRESS(ES)			10. SPONSORING/MONITORING
Armstrong Laboratory Occupational and Environmental Health Directorate Optical Radiation Division 8111 18th Street Brooks Air Force Base, TX 78235-5215			AL/OE-TR-1997-0178
11. SUPPLEMENTARY NOTES			
12a. DISTRIBUTION/AVAILABILITY STATEMENT		12b. DISTRIBUTION CODE	
Approved for public release; distribution is unlimited.			
13. ABSTRACT (Maximum 200 words)			
Seven Cynomolgus fasciculata who had graded laser lesions placed in one eye only 6 years previously were evaluated by electro-physiological recording techniques. All animal recordings were performed under IACUC approved protocols. The single q-switched pulses from a neodymium-YAG laser produced lesions of 4 types at the time of placement: no visible change, minimal visible lesions, "white dot" lesions (localized circumscribed retinal blanching) and "red dot" lesions (contained retinal hemorrhage). Single exposures had been made both foveally and at 5 degrees eccentricity in the parafovea superiorly, inferiorly and temporally. The multifocal (perimetric) electroretinogram was recorded from specialized contact lenses through hospital grade amplifiers. Optimization of recording parameters resulted in repeatable maps of the central retina. Lesions were demonstrable, especially in the foveal "red dot" cases, although the amount of signal decrement was not severe. Vernier visual evoked potentials were recorded in response to 95% contrast bars from scalp electrodes. These recordings were successful in smaller animals with less than contained retinal hemorrhage lesions in the fovea. Analysis demonstrated a significant decrease of the pattern response signal/noise in the experimental eye overall, and an apparent relative loss of vernier signal in some lesioned eyes. Animals with the more severe lesions have degraded small pattern responses and no recordable vernier response. Less obvious losses produced smaller decrements.			
14. SUBJECT TERMS		15. NUMBER OF PAGES	
ERG, healing, laser, neodymium, perimetry, primate, retina, q-switch, vernier, VEP, Wolfe grade		26	
		16. PRICE CODE	
17. SECURITY CLASSIFICATION OF REPORT		18. SECURITY CLASSIFICATION OF THIS PAGE	
Unclassified		Unclassified	
19. SECURITY CLASSIFICATION OF ABSTRACT		20. LIMITATION OF ABSTRACT	
Unclassified		UL	

THIS PAGE INTENTIONALLY LEFT BLANK

TABLE OF CONTENTS

	Page
ACKNOWLEDGMENTS.....	v
INTRODUCTION.....	1
METHODS.....	2
Subjects	2
Procedures	2
Stimuli, Recording and Data Processing.....	4
RESULTS.....	6
VEPs to Checkerboard Patterns	6
VEPs to Venier Offsets	7
ERGs to Topographic Mapping Stimuli.....	9
DISCUSSION	12
REFERENCES.....	13

LIST OF FIGURES

Figure No.	Page
1	Layout of the optical alignment systems used in study 3
2	Summed and averaged VEPs from checkerboard stimulation 7
3	Vernier VEPs from animals #cy1159 8
4	Fundus image of eye 9
5	Trace array recorded from cy1159 OD 10
6	Intensity coded map derived from the trace array of the scalar 10
7	The 3-demensional topographic representation of the ERG 11
8	Profile of relative response amplitudes through response decrement .. 11

ACKNOWLEDGMENTS

This work was supported in part by funds under USAMRMC Contract No. DAMD17-95-C-5038, Ft. Detrick, MD, by funds from TASC, Inc., Reading, MA, equipment from the Armstrong Laboratories and from the US Army Medical Research Detachment (WRAIR), both of Brooks AFB, TX, and by an unrestricted grant to the Ophthalmology department at the University of Kentucky from Research to Prevent Blindness, Inc. Dr. William Hare of Allergan Pharmaceuticals, Inc. (Irvine, California) is also gratefully acknowledged for his technical advice in this project.

THIS PAGE INTENTIONALLY LEFT BLANK

INTRODUCTION

Vision and visual compromise due to retinal burns caused by laser exposure has been evaluated and measured in many different ways. Visual field effects, changes in grating acuity, gray scale contrast sensitivity and chromatic sensitivity have all been measured in the attempt to quantitate a very complex sense system. Previous studies by both this author and many others have examined the effect of laser exposures on the electrophysiological responses of the retina.¹⁻¹⁷ In some cases, the interest was in very acute changes, while in many others, only longer term studies were possible. Long term studies on the functional recovery of the retina subjected to discrete laser lesions have not been completed, nor are most techniques available suitable for noninvasive examination of small disjunct retinal areas. Over the past few years, an innovative experimental technique has been introduced that may help to address this problem: multi-input electroretinography.^{18,19} This method uses a tiled stimulus display in which each hexagonal tile is flickered independently such that the overall averaged luminance change is zero and each tile has a unique temporal signature (the m-sequence technique). The ERG (electroretinogram) is recorded to this multiple stimulus from a single recording electrode and then cross-correlated to each tile's individual signature. This results in a topographic or perimetric map of the retinal response that seems to correlate with ganglion cell density across the retina.

A further method was employed to investigate the ability of the visual system to make localization judgments, i.e. vernier acuity, as opposed to pattern resolution judgments, e.g. grating or letter acuities.²⁰ The ability of an observer to correctly judge the offset of 2 dots or line elements is quite resistant to optical degradation and is significantly different in its response to various pathologies.^{21,22} Additionally, this ability is critical to aiming and tracking tasks common to many activities, including simply driving down the road between the lines and parking a vehicle. Visual evoked potential correlates of vernier hyperacuity have been obtained in humans.²³⁻²⁵ These studies show that the vernier visual evoked potential (VEP) in humans scales linearly with log offset and thus can permit estimation of the psychophysical vernier acuity threshold by extrapolation to signal amplitude extinction. However, vernier acuity falls off with retinal eccentricity even faster than resolution acuity or contrast sensitivity.²⁶

The animals used in this study have had graded laser lesions placed 6 years previously. The lesions were produced by the native collimated beam from a pulsed Nd-YAG laser emitting 1062 nm light without expansion or focusing by any lens system other than that of the eye itself. Placement and severity of these lesions was governed by attempts to produce "Wolfe grade" equivalent effects⁴ with single q-switched exposures. Four lesions had been placed in the right eye of each animal, the left eye serving as a normalizing control with no laser exposures. The exposure energy (and thus lesion type) was counterbalanced across both locations and animals for severity and only four exposures were made in the right eye of each animal. The acute effects of these lesions on acuity as measured by the sweep VEP technique have been previously reported.¹⁷

Summarizing the seven animals in this experiment, at the foveal site there are two animals which were labeled with no visible change at the time of exposure, two with a "minimal visible lesion" (MVL, or Wolfe Grade 1B⁴), two with "white dot" lesions (retinal blanching, grade IIB) and three with "red dot" lesions (contained retinal hemorrhage, grade IIIB). At the parafoveal locations, there are 11 sites with no visible change at the time of exposure, four sites with MVL (IA), six sites with a white dot lesion (IIA), and four sites with a red dot lesion (IIIA). Their current appearance varies and in some cases varies drastically from the grading at the time, ranging from some "red dot" lesions almost vanishing to now relatively prominent "minimally visible" lesions.

Since as noted above, the VEP falls off with eccentricity due to both cortical magnification and to the topographic mapping of the visual field on the cortex, the signal to noise ratio of the VEP will fall off drastically in any attempt to record a response from the periphery with noninvasive methods.²⁵ Accordingly, this report is limited to the examination of the vernier VEP responses when the stimulus is placed on the foveal area itself. The consideration whether isolated peripheral lesions have any additional effect to that of the foveal exposure must await a further study with different animals, although some indications are presented here. Finally, in order to identify the amount of absolute functional decrement, the retinal areas were mapped with ERG perimetry.

METHODS

Subjects

The decision of a suitable species was driven by three considerations: the animal must be a primate, it must have high luminance, high acuity color vision, and its retina must have a fovea. These requirements arise from the need to model the human visual system organization (anatomy and function) both retinally and cortically in order to generalize the results of this study to human visual performance. The lowest species that could therefore be used was the cynomolgus monkey (*Macaca fascicularis*). The animals that were used in this study have been housed in AAALAC approved facilities since their laser exposures in 1991. Further, the recording methods are noninvasive and routinely used with human patients. All procedures were pre-approved by the university IACUC and followed the guidelines of both ARVO and the NIH.

Procedures

The animal was sedated with ketamine (10 mg/kg) supplemented with acepromazine (1 mg/kg) IM, and then brought to the laboratory. The animal was anesthetized with pentobarbital IV (10 mg/kg) and muscularly relaxed with pancuronium bromide IV (0.025 mg/kg) as bolus doses.

For the VEP recordings, the pupils were dilated with 1% tropicamide and 1% neosynephrin drops. The animal then was intubated and wrapped in a warming blanket on a padded rotating stage. Temperature, ECG and pCO₂ were monitored, and ventilation and blanket temperature were adjusted to maintain stable physiologic values. EEG and ECG were monitored for signs of discomfort and the anesthetic level adjusted with backup doses as needed. The fovea of one eye was aligned in front of the fundus camera and the other eye patched closed. Each animal had been individually refracted for the stimulus distance previously and had keratometry performed to specify the appropriate contact lens parameters. This individually fitted corrective contact lens was placed on the cornea over artificial tears and the retina visualized through it. Figure 1 shows the optical layout and alignment system that was used for both VEP and ERG recordings.²⁷

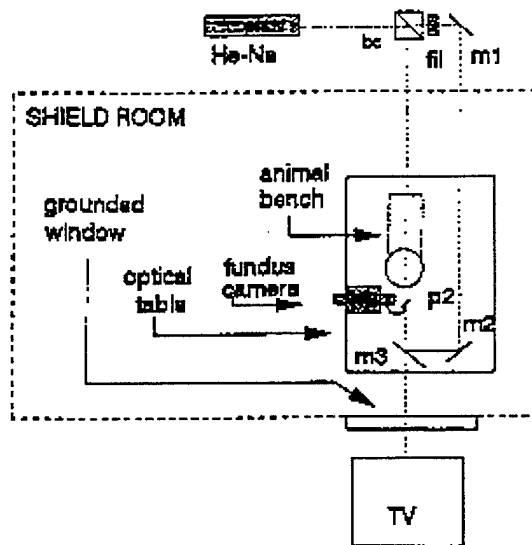


Figure 1: Layout of the optical alignment system used in this study. He-Ne: alignment laser; bc: beam splitter cube; m1, m2 & m3: mirrors (m3 can be moved from the line of sight); p2: removable 80% reflecting pellicle.

For the ERG recordings, prior to intubation and alignment, an especially constructed bipolar Burian-Allen lens was test fitted to each eye. A spherical lens was selected by streak retinoscopy to correct for the monitor to eye distance and any optical ametropia. After placing the wrapped and intubated animal on the stage and establishing a physiological steady state (pCO₂, etc.), the ERG contact lens electrode was replaced on the cornea over viscous artificial tears (GoniosolTM) and the retina visualized through it. Following alignment of the fovea with the fundus camera crosshairs, the previously individually selected correcting lens was placed in front of the contact lens to bring the monitor screen into focus on the retina, using the alignment laser back reflections for centration. ERG maps were calculated from an 8 min long m-sequence acquisition. At

least 2 and generally 4 maps were made in each eye to determine repeatability. Response data for each animal's eye was averaged over the repeated maps for final analysis.

After an experimental session, the animal was allowed to recover from the muscular immobilizing agent. When it could breathe unassisted, it was extubated, removed to the transfer cage and then returned to the colony under the supervision of the veterinary staff.

Over the duration of this seven year project, two of the nine animals originally exposed as part of a previous contract investigating acute effects of laser exposure were euthanized before their vernier VEPs and multifocal ERGs could be recorded. One was terminated on the veterinarian's recommendation due to advanced systemic illness soon after the initial exposures, and was not available for this study. A second animal developed untreatable diabetes with concurrent cataracts, and was terminated before useful data could be obtained. The data in this report therefore are based on the remaining seven animals.

Stimuli, Recording and Data Processing

The hyperacuity (vernier) stimuli were produced on a square high resolution (1024 pixels squared) monochrome monitor (VisionProbe (tm)) measuring 8.35 degrees of visual angle at the eye. The stimulus was constructed of five black vertical bars 2.63 degrees tall on a white background (78 Foot-Lamberts) whose center third was horizontally offset and subsequently realigned 694 msec later (0.72 Hz), following the method of Levi *et al.*²³ A gap of 2 pixels (0.97 arcmin) was placed between each third. Each bar measured 9 pixels (4.4 arcmin) in width and was separated from its neighbors by a further 9 pixels producing an overall pattern width of 81 pixels (0.66 deg). Contrast was measured at 99.6%. The offset was counterphased between 0 and (in turn) 27, 18, 9, 4, and 2 pixels to evoke the VEP, thus covering a range from a maximum of 13.2 arcmin (approx. 0.24 degrees) down to 0.98 arcmin. The VEP was recorded from bilateral occipital scalp electrodes over the foveal visual cortex individually referenced to the eyebrows (the central scalp served as signal common) in response to the each stimulus until the step size used evoked no recognizable response (generally around the 9 pixel shift size). In order to avoid any time locked activity that might obscure the signal, a random 0-500 msec dither was introduced between each 1 second stimulus epoch. In most cases, at least 800 sweeps acquired over multiple runs had to be averaged together and the two cortical channels from each animal combined in order to get a response with sufficient signal under these anesthetic and recording conditions. In addition, a set of control recordings with 8 shift/sec counterphasing 99.6% contrast checkerboard stimuli at 1, 3 and 10 cycles/degree filling the entire monitor were used to estimate the overall visual response from each eye.

The steady state (8 Hz) checkerboard VEPs were underwent Fourier analysis and the strength of the 8 Hz component was recorded. This power spectral density, being

bounded at 0, was log transformed into a normal distribution before the analysis of variance (repeated measures ANOVA by CSS Statistica, Statsoft Inc., Tulsa, OR). Signal to noise ratios (s/n) were constructed from the power of the peak pattern response divided by the average power in the 2 neighboring frequency bins. Since these ratios also are bounded at 0, they were log transformed before analysis. Next, in order to create a standard comparison template, all vernier evoked potentials were normalized to the individual animal's control eye base recording (the 27 pixel shift). The averaged normalized vernier VEPs were evaluated by cross correlation limited to the time region in which the vernier component occurred (between 186 ms to 250 ms, containing the nominal P200-N220 response) both to this average template, and also between each eye for each animal. The strongest positive correlation coefficient (a Pearson's r) at the closest offset (τ) to the template response was chosen to characterize the response, i.e. the closest local maximum r to $\tau=0$. Additionally, the correlation coefficient at $\tau=0$ was also noted. Since correlation coefficients are not normally distributed, they also had to be transformed via the equation (known as a Fischer's transformation):²⁸

$$x(r) = 0.5 \ln((1+r)/(1-r)). \quad (1)$$

From this, means and standard deviations based on the variable x can be determined, since x is approximately normally distributed. These transformed values were then compared by repeated measures ANOVA and the effects of the lesions extracted. For graphical purposes, normal ranges can be obtained with these values (e.g. means ± 2 S.D.), and then back transformed to provide normal boundaries on a graph of r vs τ (the lead/lag amount) via the inverse of equation 1 as follows:

$$r = 1 - 2 / (\exp(2x) + 1). \quad (2)$$

These equations coupled with the cross correlation analysis provide an relatively objective method of statistically determining the presence of any reliable response (i.e. the VEP), rather than having to judge which squiggle is the actual response component.

VEPs were recorded to contrast reversing checkerboards and to a repeatedly occurring lateral offset and realignment of the vernier pattern. One of the animals (12043, a large male) had pattern VEPs in the control eye which at the base stimulus (1 c/d checkerboard) were too small to be useful; this animal's data was eliminated. Further, two other animals (1209 and 12029) had no reliable vernier VEPs even to the largest offset in the control eye (correlation coefficients with the template were consistently negative) and so were dropped from the vernier analyses. In order to attempt a statistical analysis with the remaining few animals, the experimental eyes were grouped roughly as those with no lesions to minimally visible foveal lesions (two animals), and those with severe or scarring foveal lesions (two animals). All comparisons were made against their paired control eye (repeated measures ANOVA). Both the $x(r)$ at $\tau=0$ and the $x(r)_{\text{max}}$ with the coupled τ at $x(r)_{\text{max}}$ as a covariate were analyzed as a function of lesion class (minimal vs white or red dot) with both eye and offset as the repeated measures.

Multifocal ERGs were recorded to a 16 degree diameter pattern of packed equal area hexagons centered on the fovea. The multifocal ERG stimulus was produced by a specially designed Nu-Bus video board hosted in a Macintosh Quadra 650 computer. Two multi-sync monitors are attached (one 14 inch stimulus monitor and one console monitor) and data was acquired by an analog to digital converter also housed in the same computer. The raw signal was recorded from corneal contact lens electrodes and preamplified with hospital grade amplifiers before being fed to the computer. Amplifiers were set to a gain of 200,000 with a bandpass of 3 - 100 Hz. The specially written software package (VERISTM) simultaneously updates multiple areas on the stimulus monitor while synchronously acquiring the electrophysiological data and calculating the next m-sequence set. This system is available from the developer, Dr. Erich Sutter (Smith-Kettlewell Eye Research Institute, 2232 Webster St., San Francisco, CA 94115). Each retina was mapped with a 61 element, equal area hexagonal stimulus pattern placed at 81.3 cm. This arrangement resulted in approximately 1.5 deg resolution in the 16 deg diameter perimetric maps. Using software interpolation, the resolution essentially can be doubled.

Ocular photography included both color fundus pictures of each exposed eye, and an associated fluorescein angiogram (FA). For the FA sessions, muscular relaxation via pancuronium bromide was not used, and only the ketamine/acepromazine IM sedation and pentobarbital IV anesthesia at the standard doses was employed. Depending on the animal's size, between 0.25 and 0.5 ml of 10% sodium fluorescite was injected IV for the imaging study.

RESULTS

VEPs to Checkerboard Patterns

Figure 2 shows the normalized summed averages series of VEP responses from the normal control eyes (OS) and from all the fellow laser exposed eyes (OD) elicited by 3 checkerboard stimuli of differing check sizes. As can be seen, the lesioned side has pattern VEP responses down to 10 cycles per degree that appear similar to the control eye. Despite the small number of animals, statistical analysis of the signal to noise ratios derived from the power spectral densities of the steady state pattern VEPs showed that as a class, the more severely exposed eyes have lower log(s/n) than the normal eyes ($P=0.036$); however overall response power itself was not significantly different as a function of either eye, or exposure class. There was a tendency towards more severe effects with more severe lesions, but this did not attain significance ($p=0.27$). Spatial frequency was as expected a significant factor ($P=0.005$) with the lowest spatial frequency demonstrating a stronger (larger) response than the smaller patterns, i.e. a tuning curve.

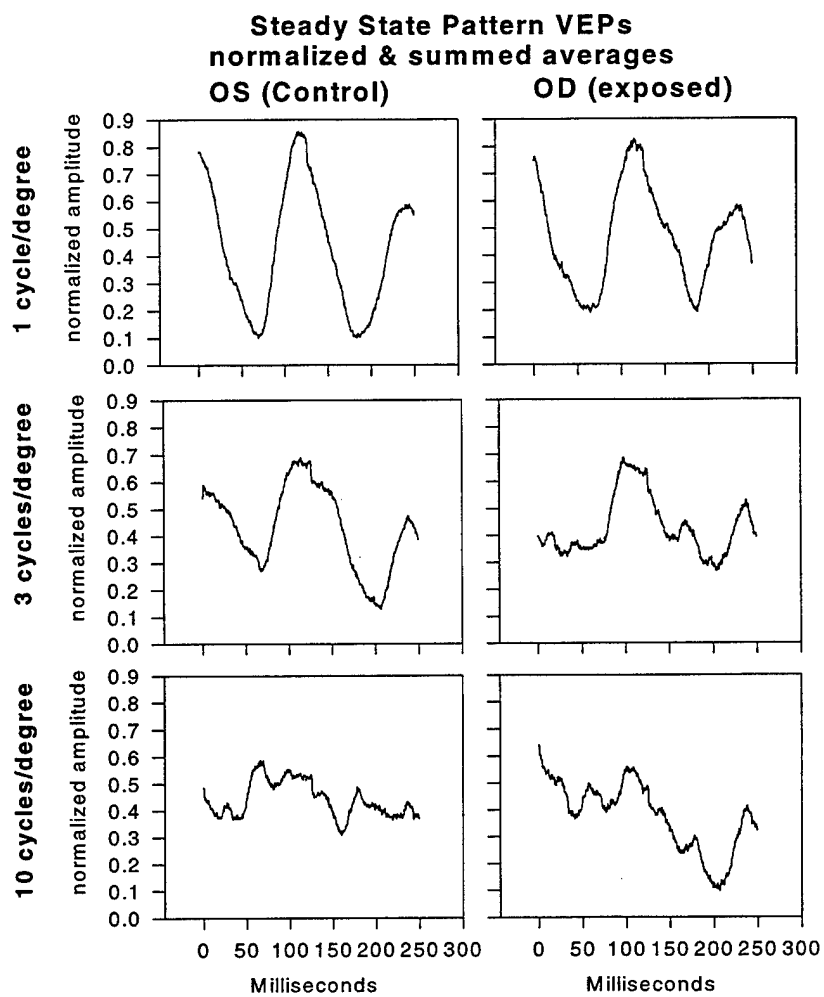


Figure 2. Summed and averaged VEPs from checkerboard stimulation. Data combined across all animals.

VEPs to Vernier Offsets

Figure 3 shows foveal vernier VEP responses from one animal, demonstrating that even with large offsets, the response decreases in the lesioned eye while remaining recordable from the control eye.

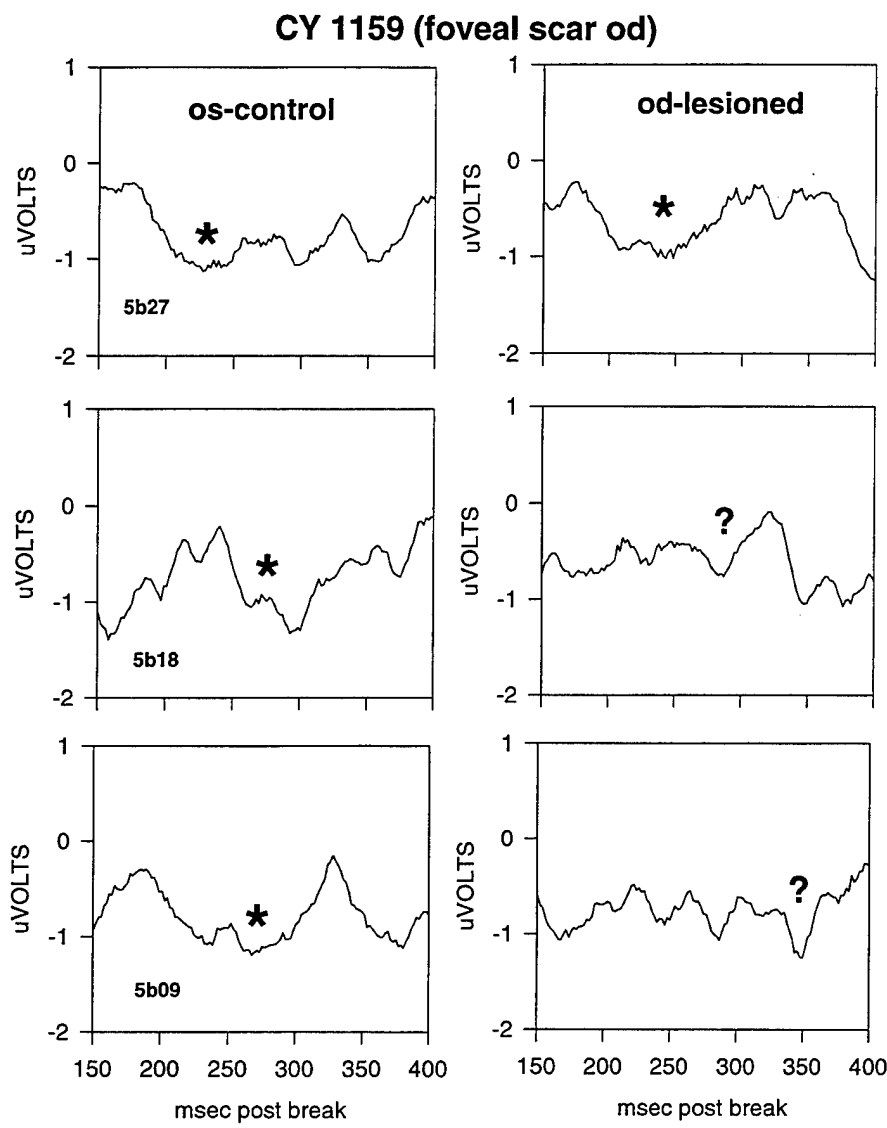


Figure 3. Vernier VEPs from animals # cy1159, which had an apparent bridging foveal scar OD. The asterisk marks the vernier VEP; the question mark indicates a possible response.

Analysis of the maximum crosscorrelation results (with the corresponding tau as a covariate) demonstrated no significant effects due to eye, class or vernier offset, even though the trends were as expected (lower correlation with smaller offsets, in the lesioned eye and with more severe lesions). For example, comparison of the data between exposure classes (minimal vs white or red lesions) in the experimental eye demonstrated

a tendency towards more severe losses of correlation with the more severe lesion, but the effect did not attain significance ($p=0.152$). In contrast, examination of the correlation results with no offset in time showed an interaction effect between lesion class and eye ($p=0.041$). Looking at only the exposed eye and analyzing for the effect of lesion class across all vernier offsets, the more severe lesion was significantly more effective in dropping the response ($p=0.033$). Finally, there is a tendency for the interocular correlation to drop with the more severe lesions, but this did not attain significance in this small sample ($p=0.13$). A related finding was that off-axis burns (approx. 5 degree eccentricity) did not seem to affect central vernier acuity in these particular long term animals, e.g. one animal with an apparent MVL in the fovea but with white and red dot lesions in periphery has vernier VEP responses that were not significantly different between the control and exposed eye.

ERGs to Topographic Mapping Stimuli

All ERG maps of eyes with obvious discrete lesions showed remarkably small circumscribed areas of somewhat reduced response, even in those retinas noted as having “red dot” lesions at the time of placement. The most severe drop was of approximately 25% in one eye with an apparent bridging scar between the foveal site and the superior site (animal # cy1159, vernier VEP in Figure 3, above). Figure 4 shows the fundus image of this eye (immediately below), Figure 5 the trace array, and Figure 6 the coded map (gray scale in this paper).

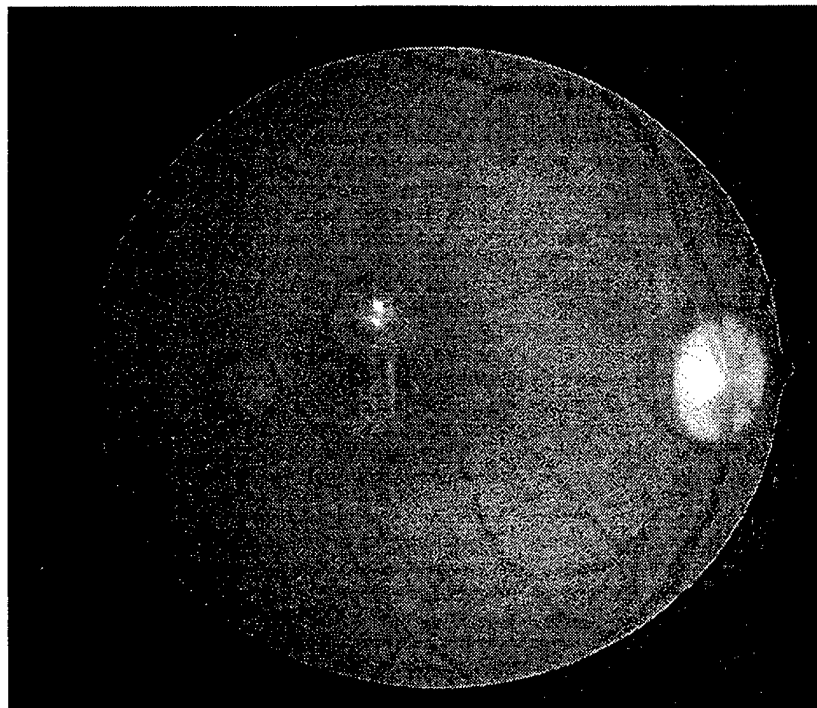


Figure 4. Fundus image of the eye of cy1159.

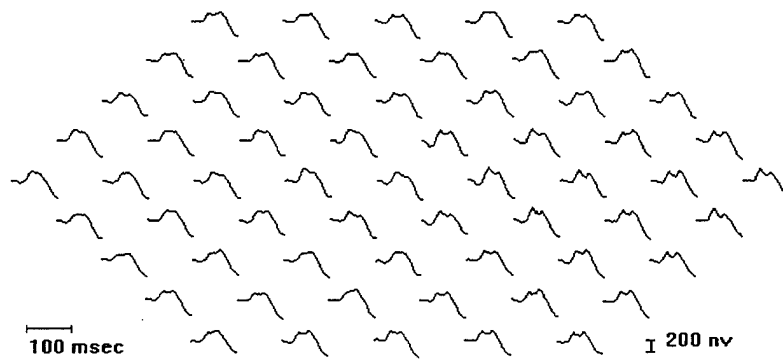


Figure 5. Trace array recorded from cyl1159 OD.

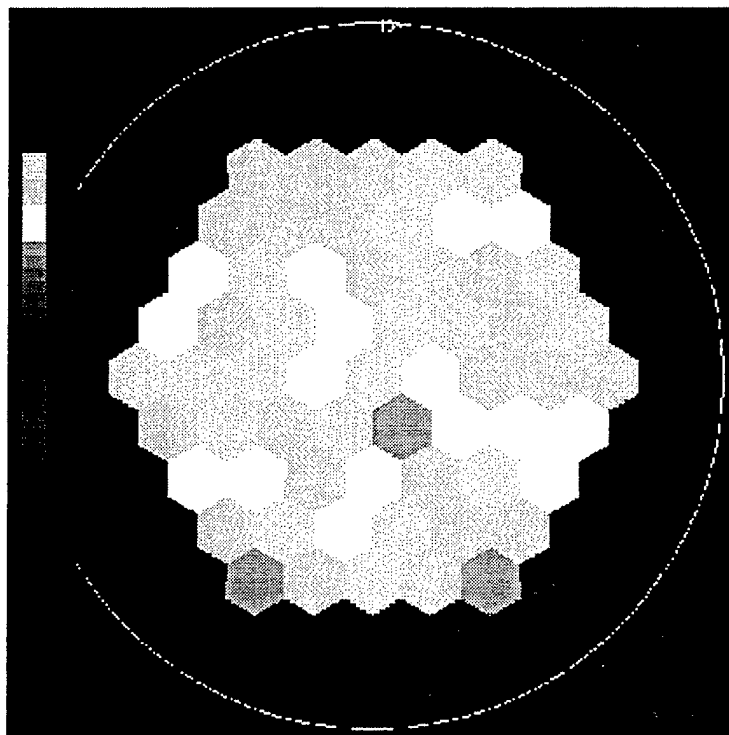


Figure 6: Intensity coded map derived from the trace array of the scalar product showing the point of maximum signal decrement.

Visually, the 3-dimensional maps appeared to be volcano shaped rather than showing a more or less smooth hill of vision. The caldera of this volcano averaged about a 10% drop in response compared to the areas immediately adjacent. Figure 7 (below)

shows the 3-dimensional topographic representation of the ERG responses and Figure 8 shows a profile of relative response amplitudes through the response decrement, and demonstrates the above mentioned 25% drop.

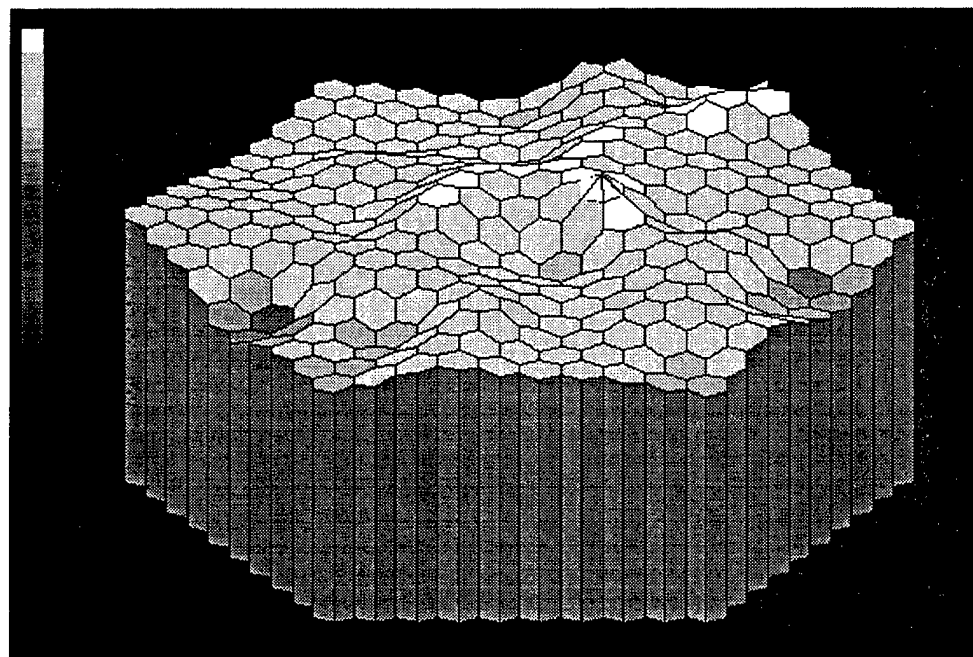


Figure 7. The 3-dimensional topographic representation of the ERG responses

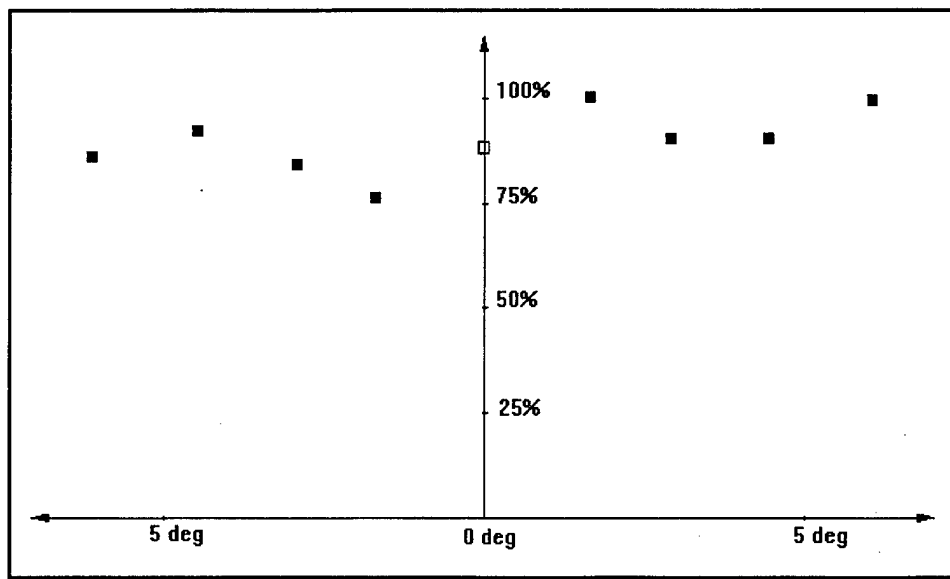


Figure 8. Profile of relative response amplitudes through the response decrement, and demonstrates the above mentioned 25% drop.

Most of the maps also showed some edge artefacts (loss of signal), especially in the inferior field that may have been due to partial occlusion of the upper edge of the pupil by the central recording element in the contact lens. As a result, mapping of the peripheral lesions may have to be done explicitly. Lesions of the MVL type were not clearly apparent in these maps, nor were all the white dot type lesions.

DISCUSSION

The decrease in signal to noise ratio in the relatively large field pattern VEPs without a concomitant loss of absolute response power is intriguing. Does an abnormal fovea actually increase the visual system's noise as opposed to simply removing its contribution to the response? This type of masking or interference may have functional consequences that extends beyond the apparent lesion diameter, and would need to be separately considered. On the other hand, the data presented here does not support the inverse idea, viz. that damaged peripheral retina has a significant ability to affect foveal function as measured by pattern VEP.

The comparison between the responses to checkerboard stimuli and vernier stimuli of a comparable size indicates that the vernier response is probably even more sensitive to retinal disruption, a finding in opposition to that noted with optical compromise. This might be expected, since the pattern VEP responses were obtained with stimuli that covered normal as well as abnormal retina, but the localized vernier stimuli may not have impinged on unexposed retina, and in the case of the most severe lesions, may not have extended outside a presumed local scotoma. A similar study demonstrated essentially full recovery of threshold grating acuity within 2 weeks of a hemorrhagic retinal lesion in the fovea when measured with gratings larger than the lesion diameter.²⁹ This study confirms that such recoveries may be stable. Other data exists that implicates retinal ganglion cells as being the limiting factor in vernier resolution.³⁰ While this data was obtained in cats rather than primates, if the physiological mechanism holds across species, the apparent damage to vernier acuity with the current laser lesions implies that the cortex may not be able to compensate for these retinal signal losses, unlike the image filling in or illusory border completion that can occur with more extended patterns.³¹ In summary, the vernier VEP analyses imply that for any offset size, including those well above normal vernier threshold, 1) there tends to be a drop due to any foveal exposure, and 2) this drop appears to be more severe with greater lesions.

It should be reiterated that not all animals produced recordable vernier VEPs with this protocol, even from their normal eyes. This tended especially to be the case for the larger (male) animals and may be an artefact of their greater skull thickness and head musculature combined with the small size of the signal when recorded by surface (either subcutaneous needle or scalp cup) EEG electrodes. In order to improve this situation, implantation of chronic electrodes to record from at least the dural surface if not trans cortically probably would be required.³² Finally, an exhaustive perilesional mapping protocol in order to maximize any vernier signal by placing it just outside of a (presumed)

lesion scotoma was not undertaken. Behavioral studies which would allow the animal to adopt individual compensatory strategies (such as off axis viewing with alternate preferred retinal loci) might be more appropriate to determine the final functional consequences of discrete retinal lesions such as those in this study.

In contrast to the previous report of results with these animals using the ERG mapping technique,³³ further work has shown that there are three prerequisites for successful recording: 1) good oculostasis, insured by pentobarbital and pancuronium bromide medication, 2) a well fitted nonglaring bipolar ERG contact lens with the correct contact lens curvature as well as acceptable electrical and optical properties, and 3) refraction by streak retinoscopy over the contact lens to correct both for the stimulus distance and the animal's own refractive error, if any, as well as for the lens induced changes.

It should be noted that each retinal map took 8 minutes to acquire, and several maps were averaged to obtain the data. Some eye drift was bound to occur since the recordings were not made under optically stabilized conditions, nor under infrared visual monitoring. Consequently, the response profiles may be somewhat shallower and the actual limits of the response losses less distinct than may be in fact the case. However, this drift could only have been on the order of a few degrees since the alignment was checked before and after the series of runs, and in most cases seemed stable to visual inspection. Nevertheless, that there is as much signal as was seen in these cases implies that these focal lesions do not have a wide spread effect on the entire retina, nor that all luminance processing close by, if not at, the lesions site is destroyed. Whether this retention of signal generating ability is due to the healing process, e.g. photoreceptor migration into the lesion site, must await histological recovery of the tissue.

A final point concerns the possibility of deeper functional deficits in the maps when the visual system is queried with more demanding stimuli, e.g. patterns. This could be done electrophysiologically with the visual evoked potential (VEP). The few VEP test maps that were obtained seemed to indicate that VEP perimetry can demonstrate lesions that are not apparent by luminance ERG. Further work will be needed to determine the extent of deficit at this level of the visual system.

REFERENCES

1. Moshos M. ERG and VER findings after laser photocoagulation of the retina. *Metab Pediatr Ophthalmol* 6:101 (1982).
2. Fowler BJ. Accidental industrial laser burn of the macula. *Ann Ophthalmol* 15:481 (1983).
3. Boldrey EE, Little HL, Flocks M, Vassiliadis A. Retinal injury due to industrial laser burns. *Ophthalmol (Rochester)* 88:101 (1981).
4. Wolfe JA. Laser retinal injury. *Mil Med* 150:177 (1985).

5. Stuck BE, Lund DJ, Beatrice ESW. Repetitive pulse laser data and permissible exposure limits. Presidio of San Francisco, CA: Letterman Army Institute of Research. Institute Report No. 59 (1978).
6. Gibbons WD, Allen RG. Retinal damage from suprathreshold Q-switch laser exposure. *Health Phy* 35:461 (1978).
7. Allen RG, Thomas SJ, Harrison RF, Zuglich JA, Blankenstein MF. Ocular effects of pulsed Nd laser radiation: variation of threshold with pulsedwidth. *Health Phy* 49:685 (1985).
8. Merigan WH, Pasternak T, Zehl D. Spatial and temporal vision in macaques after central retinal lesions. *Invest Ophthalmol Vis Sci* 21:17 (1981).
9. Callin GD, Devine JV, Garcia P. Visual compensatory tracking performance after exposure to flashblinding pulses: I, II, III. USAF School of Aerospace Medicine, Brooks Air Force Base, TX: Reports SAM-TR-81-3, -7, -8 (1981).
10. Randolph DI, Schmeisser ET, Beatrice ES. Grating visual evoked potentials in the evaluation of laser bioeffects: twenty nanosecond foveal ruby exposures. *Am J Optom Physiol Opt* 61:190 (1984).
11. Schmeisser ET. Flicker electroretinograms and visual evoked potentials in the evaluation of laser flash effects. *Am J Optom Physiol Opt* 62:35 (1985).
12. Schmeisser ET. Laser flash effects on laser speckle shift VEP. *Am J Optom Physiol Opt* 62:709 (1985).
13. Schmeisser ET. Schmeisser ET. Laser induced chromatic adaptation. *Am J Optom Physiol Opt*, 65: 644-652 (1988).
14. Previc FH, Blankenstein MF, Garcia PV, Allen RG. Visual evoked potential correlates of laser flashblindness in rhesus monkeys. I. Argon laser flashes. *Am J Optom Physiol Opt* 62:309 (1985).
15. Previc FH, Allen RG, Blankenstein MF. Visual evoked potential correlates of laser flashblindness in rhesus monkeys. II. Doubled neodymium laser flashes. *Am J Optom Physiol Opt* 62:626 (1985).
16. Glickman RD, Previc FH, Cartledge RM, Schmeisser ET, Zuglich JA. Assessment of visual function following laser lesions. USAFSAM Protocol # 7757-02-82 (Contract F33615-84-C-0600) (1986).
17. Schmeisser ET. Acute laser lesion effects on acuity sweep VEPs. *Invest Ophthalmol Vis Sci*, 1992; 33:3546-3554.
18. Sutter EE, Tran D. The field topography of ERG components in man - I. The photopic luminance response. *Vis Res* 32:433 (1992).
19. Bearse MA, Suter EE. Imaging localized retinal dysfunction with the multifocal electroretinogram. *J Opt Soc Amer A* 13:634 (1996).
20. Westheimer G. Visual acuity and hyperacuity: resolution, localization, form. *Am J Optom Physiol Opt* 64:567-574 (1987).
21. Enoch JM, Williams RA. Development of clinical tests of vision: Initial data on two hyperacuity paradigms. *Percept Psychophys* 33:314-322 (1983).
22. Enoch JM, Essock EA, Williams RA. Relating vernier acuity and Snellen acuity in specific clinical populations. *Doc Ophthalmol* 58:71-77 (1984).
23. Levi DM, Manny RE, Klein SA, Steinman SB. Electrophysiological correlates of hyperacuity in the human visual cortex. *Nature* 306:468-470 (1983).

24. Steinman SB, Levi DM, Klein SA, Manny RE. Selectivity of the evoked potential for vernier offset. *Vis Res* 25:951-961 (1985).
25. Srebro R, Osetinsky MV. The localization of cortical activity evoked by vernier offset. *Vis Res* 27:1387-1390 (1987).
26. Enoch JM, Williams RA, Essock EA, Barricks M. Hyperacuity perimetry. Assessment of macular function through ocular opacities. *Arch Ophthalmol* 102:1164-1168 (1984).
27. Blankenstein MF, Previc FH. Approximate visual axis projection for the rhesus monkey using a fundoscope and alignment laser. *Vis Res* 25: 301-305, (1985).
28. Kendall MG, Stuart A. The advanced theory of statistics, Vol 1. Hafner Publ Co., New York, NY, pp 390-392 (1963).
29. Rhodes JW, Garcia PV. Grating visual acuity following hemorrhagic foveal lesions. *Lasers & Light* 7: 153-165 (1996).
30. Shapley R, Victor J. Hyperacuity in cat retinal ganglion cells. *Science* 231: 999-1002, (1986).
31. Ringach DL, Shapley R. Spatial and temporal properties of illusory contours and amodal boundary completion. *Vis Res* 36: 3037-3050, (1996).
32. Schmeisser ET. Laser induced chromatic adaptation. *Am J Optom Physiol Opt*, 65: 644-652 (1988).
33. Schmeisser ET. Evaluation of retinal laser lesion healing by perimetric electroretinography. *SPIE Proceedings*, 2674: 108 (1996).